

Formation of Thin Continuous Films from Isolated Nuclei

E. Bauer, A. K. Green, and K. M. Kunz
Michelson Laboratory, China Lake, California

and

H. Poppa
General Dynamics-Convair, San Diego, California

ABSTRACT

35727

The rigid model of the film growth is discussed and the results of in-situ investigations are reviewed. The generality of the conclusions drawn from in-situ experiments is examined by a discussion of the influence of the experimental conditions (the effects of the electron beam, the residual gases, the substrate surface conditions, and the film and substrate materials), and by an analysis of the growth of f.c.c. metals on alkali halides. In the final discussion the most striking phenomena observed in the formation of thin continuous films from isolated nuclei are considered from the theoretical point of view.

I. INTRODUCTION

Thin films can grow by several mechanisms shown in Fig. 1:¹ The Volmer-Weber mechanism in which 3-dimensional nuclei are formed, which grow sideward and outward until a continuous film is formed, the Frank-van der Merwe mechanism, in which the film grows monolayer by monolayer and the Stranski-Krastanov mechanism in which first a mono- or multilayer of the film material or of a mixture between film and substrate material is formed, on top of which

FACILITY FORM 602

N66 35727

(ACCESSION NUMBER)

(PAGES)

41
CR-68778

(NASA CR OR TMX OR AD NUMBER)

(THRU)

(CODE)

26

(CATEGORY)

653 July 65

Microfiche (MF) 150

Hard copy (HC) 200


CFSTI PRICE(S) \$

GPO PRICE \$

3-dimensional crystals grow. This paper is concerned with the processes which take place between the formation of 3-dimensional nuclei and the formation of a continuous film. The nucleation process itself is discussed in several other papers in this conference. The growth processes in thicker films have been reviewed recently.^{2,3} We will be concerned mainly with the kinetics of the film formation and will only briefly discuss some of the energetic aspects. Our problem can be formulated essentially as follows: Given a surface and a system of small particles, which interact with the surface and with each other, what is the structure of the film consisting of these particles? We can consider two extreme cases. In one case the particles interact strongly with each other, but only weakly with the surface, just like droplets with high surface tension which do not wet the surface. When such particles contact each other they will form one larger particle and lose their identity in this way ("liquid like behavior"). No thin continuous film can be formed, but one or several large isolated particles. In the other extreme case the particles interact so strongly with the surface and so weakly with each other that upon their contact they simply stop their sideward growth ("rigid model"). Most real situations are between these extreme cases.

II. THE RIGID MODEL

This model is easily amenable to formal mathematical treatment if it is assumed that nucleation is completely at random.⁴ The treatment is similar to that given by Avrami⁵ for the kinetics of crystallization in 3 dimensions. It leads to relations between the experimentally measurable quantities and the basic parameters determining the film growth. Such measurable quantities are:



(1) the particle distribution function $N(f, g, \xi_i, t)$ which is the number of particles with cross-section f consisting of g atoms or molecules at the time t . The other parameters ξ_i characterize, e.g. the shape of the particle, its orientation and the kind of nucleation center if preferred nucleation sites exist; (2) the fraction $F(t)$ of the surface covered with particles; (3) the total number $N(t)$ of particles; (4) the number $N'(f)$ of separated particles; (5) the number $N(f, t)$ of particles with interface size f ; (6) the number $G(t)$ of condensed atoms or molecules; and (7) the mean and differential condensation coefficients $K(t), k(t)$. These quantities can be expressed as function of:

(1) the nucleation probabilities $I(f), J_M(f), J_L(f)$ on a smooth surface, on a point-like nucleation center and on a line-shaped nucleation center respectively; (2) the lateral and normal growth rates \tilde{f} and \dot{h} of the crystals when not impeded by neighboring crystals, and (3) a system of parameters γ characterizing the crystal shape. These parameters again depend upon the vapor flux N_D , the substrate temperature T , the heat of adsorption ΔH_a and the activation energy for surface diffusion ΔH_d of the vapor molecules on the substrate, the specific free surface and interfacial energies $\sigma_s, \sigma_c, \sigma_I$, the numbers M and length L of point-like and line-shaped nucleation sites and upon other parameters such as residual gas pressure and composition, electron beam current density and energy.

The formulae for some of the measurable quantities in terms of the first set of parameters are given in Table I for nucleation on a surface without preferred nucleation sites.

TABLE I

$$(1) F(t) = 1 - e^{-\tilde{F}(t)}$$

$$(2) N(\xi_i, t) = \sum_i \int_{t'=0}^t I(\xi_i, t') (1-F(t')) dt' = \sum_i \int_{t'=0}^t I(\xi_i, t') e^{-\tilde{F}(t')} dt'$$

$$(3) N'(\xi_i, t) = e^{-\tilde{F}(t)} N(\xi_i, t)$$

$$(4) N'(f, \xi_i, t) = - \frac{I(\xi_i, t') e^{-\tilde{F}(t')}}{\frac{\partial}{\partial \tau} f(\xi_i, t, t')}$$

$$(5) G(t) = \sum_i \int_{t'=0}^t I(\xi_i, t') \gamma(\xi_i, t, t') h(\xi_i, t, t') f(\xi_i, t, t') dt'$$

$$(6) K(t) = \frac{1}{N_D} \frac{G(t)}{t}$$

$$(7) k(t) = \frac{1}{N_D} \frac{dG(t)}{dt}$$

where

$$\tilde{F}(t) = \sum_i \int_{t'=0}^t I(\xi_i, t') \tilde{f}(\xi_i, t, t') dt'$$

with

$$\tilde{f}(\xi_i, t, t') = \int_{\tau=t'}^t \frac{\partial \tilde{f}}{\partial \tau} (\xi_i, \tau, t') d\tau = \int_{\tau=t'}^t \tilde{f} d\tau ;$$

$$f(\xi_i, t, t') = \int_{\tau=t'}^t e^{-\tilde{F}(\tau)} \frac{\partial \tilde{f}}{\partial \tau} (\xi_i, \tau, t') d\tau; h(\xi, t, t') = \int_{\tau=t'}^t \frac{\partial h}{\partial \tau} (\xi_i, \tau, t') d\tau = \int_{\tau=t'}^t h d\tau.$$

\tilde{F} , \tilde{f} are the areas which would be obtained if the particles would grow unimpeded by their neighbors. I is the nucleation probability per unit area of uncovered surface. Similar expressions can be given for preferred nucleation at a finite number of sites. In general the nucleation probabilities I , J_M , J_L and the growth rates \tilde{f} and \dot{h} as well as the crystal shape parameters γ are time dependent and nucleation on the flat surface occurs simultaneously with nucleation on steps, corners and other preferred sites. This leads to very complicated expressions; therefore only greatly simplified cases have been calculated. Some typical results are shown in Fig. 2, together with experimental results by Walther⁶ on the condensation of Hg on polycrystalline Ni. In the calculation it was assumed that nucleation takes place only at a limited number M_0 of nucleation sites, and that all parameters are constant except f . Note the maximum and minimum in the differential condensation coefficient k and the coincidence of the maxima of k and N' in qualitative agreement with experiment.

In the case of nucleation on a limited number of sites N' reaches its maximum when $F \approx \frac{1}{16}$; however when nucleation can take place everywhere on the surface N'_{\max} is at $F \approx \frac{1}{4}$. A determination of the coverage F at the maximum of N' gives therefore information on the nucleation mechanism. As long as $F(t) \ll 1$ we can put $e^{-\tilde{F}(t)} \approx 1$ and obtain from Eqs. (2) and (4) in Table I, the following two simple expressions for the nucleation probability

$$I(\xi_i, t) \approx \frac{dN(\xi_i, t)}{dt} \approx \frac{dN'(\xi_i, t)}{dt} \quad (2a)$$

$$I(\xi_i, t') \approx -N(f, \xi_i, t) \frac{\partial}{\partial t'} f(\xi_i, t, t') \approx -N'(f, \xi_i, t) \frac{\partial}{\partial t'} \int_{\tau=t'}^t \frac{\partial \tilde{F}}{\partial \tau}(\xi_i, \tau, t') d\tau. \quad (4a)$$

If $\frac{\partial \tilde{f}}{\partial \tau} = \text{const} = \tilde{f}_0$, (4a) simplifies to

$$I(\xi_1, t') \approx N'(f, \xi_1, t) \tilde{f}_0 \quad \text{with } f = (t-t')\tilde{f}_0 \quad (4b)$$

$I(\xi_1, t')$ can therefore be determined in two ways: from the total number of particles as a function of time, or from the particle size distribution function at a time $t = t' + \frac{f}{\tilde{f}_0}$ if the lateral growth rate of the particles is constant and $F \ll 1$. The first approach was used in the study of the epitaxy of LiF on several alkali halides as a function of substrate temperature and deposition rate.⁷ Replicas like the one shown in Fig. 3 were taken at different film thicknesses obtained with the help of a shutter. However, the number of experimental points was insufficient and their scatter too large for meaningful results on the time dependence of $I(\xi_1, t)$ to be obtained. Poppa,⁸ in a much more refined study of the growth of Ag on amorphous carbon at 425°C in the electron microscope, succeeded in obtaining more points with much less scatter. He used both methods to determine $I(t)$ and his results are shown in Fig. 4, which gives the particle size distribution function, $N'(t)$ as measured directly and as calculated from the distribution function, and shows surprisingly good agreement. The $I(t)$ derived from N' as given in Fig. 4b using Eq. (2a) is

$$I(t) = \frac{\pi}{2} \frac{N'_{\text{max}}}{t_{\text{max}}} \sin\left(\pi \frac{t}{t_{\text{max}}}\right)$$

indicating a time lag for nucleation. More recently, Poppa⁹ has studied the growth of Sb on amorphous carbon over at temperature and particle flux range which covers nucleation with and without time lag. The early part of the film growth before N' reaches its maximum has thus been demonstrated to give valuable information on the nucleation process.

III. THE AGGLOMERATION PROCESS: THE LIQUID-LIKE BEHAVIOR

We turn now to the question of how far reality deviates from the rigid model. In 1942, Hass¹⁰ had already noticed that with increasing thickness the particles of a Ag film coalesced into larger particles indicating that the rigid model was only a very rough approximation. His observations were later confirmed for many other systems, but the most striking evidence came from in-situ film growth in electron microscopes which allowed the continuous observation of the film growth. Such experiments have been performed for the systems given in Table II.

TABLE II

FILM	SUBSTRATE	CONDENSATION RATE Å/min	SUBSTRATE TEMP. (°C)	REFERENCES
(1) Amorphous Substrates				
Ag, Au, Sn	Formvar		20	11
Ag	Carbon	1 - 500	250, 425	8, 15, 17
Au	Carbon	20		17
Cu	Carbon	1 - 500	250	15
(2) Single Crystal Substrates				
Ag	MoS ₂	1 - 500	250 - 450	12, 13, 15, 17, 18, 20, 21
Ag	Mica	20 - 500	300, 450	16, 20
Ag	Graphite	1 - 10		12, 15
Ag	{111} Au, {111} Pt	20 - 500	450	20
Au	MoS ₂	20	300 - 400	17, 21
Au	{111} Ag	50	450	14
Au	{111} Pd	20 - 500	200, 450	20
Cu	Graphite	1 - 10		15
Pd	{111} Au	20 - 500	50, 200, 450	20
Pb	MoS ₂			19

While the results of these investigations vary widely with film and substrate material, substrate temperature, condensation rate, surface condition and residual gas, they show a number of common features of which the most striking one is the liquid like behavior of the crystalline film particles. Neighboring particles with well defined crystallographic shapes suddenly coalesce to form one larger particle with rounded profile which on further growth develops a crystallographic form again. At present it is not certain whether actual contact of the sideward growing particles is necessary for coalescence or if coalescence can also occur by a sudden finite relative motion of separated particles. Figure 5a shows one micrograph out of a series taken during deposition of Ag onto mica at 450°C. Figure 5b is a superposition of the crystal shape in 3 growth stages from this series. Figure 6 shows a coalescence sequence for Ag on MoS₂. Better than any description is the liquid like behavior illustrated by cinefilms. (A short presentation of a cinefilm of the growth of Ag on MoS₂ taken by H. Poppa follows.)

The tendency to coalescence of Ag crystals on various substrates decreases from graphite to mica to MoS₂ to {111} Au and {111} Pt. At the same time the tendency to sideward growth increases indicating, increasing film-substrate interaction. On graphite nucleation is strongly preferential and 3-dimensional, while on the metals given in Table II, initial growth is mainly 2-dimensional (alloying!); 3-dimensional crystals are formed only on top of the initial layer and show little tendency to coalescence. Pashley et al.²¹ have made some qualitative considerations of the coalescence mechanism using the theory of sintering of spherical particles. They found that both volume and surface diffusion can account for the rapid change in particle shape during coalescence with surface diffusion being the most probable process. While the mechanism of

coalescence is not completely understood at the present time, there is little doubt that the driving force for it is surface and interfacial energy. The larger the surface and/or the interfacial energy as compared to the substrate surface energy, the stronger the tendency to coalescence. High surface mobility also encourages coalescence. The agglomeration process in the growing film is therefore determined to a large extent by the same parameters which determine nucleation. It is this fact, little appreciated in the past, which makes the study of the agglomeration stage so important for the understanding of the structure of continuous films. We will come back to this later.

Some other important observations of in-situ studies should be mentioned. When particles with different orientations coalesce, the resulting particle in general is again a single crystallite, provided the merging particles or at least one of them was not too large ($< .1 - 1 \mu$ in the systems investigated). This is true both for amorphous substrates, e.g. for Ag on carbon¹², and for single crystal substrates, e.g. for Ag on MoS₂,²¹ where particles which are in twin position to one another frequently assume one of the two positions upon merging. As a consequence of these processes it is not possible to calculate any of the previously discussed quantities N , N' , F , etc. using the rigid model if the merging particles are small which is the case for most evaporations. Only at very low supersaturation can we expect the rigid model to be applicable. Before coalescence the isolated crystals frequently rotate during growth; rotations, random in time, direction and magnitude up to 3° have been observed for Ag crystals growing on MoS₂.¹² For more details we refer to the original work (8, 9, 11-21).

The experimental conditions of in-situ investigations have been improved considerably from the experiments of McLaughlan et al., 15 years ago, in which

the vacuum was poor, the evaporation rate was not controlled and the growing film was contaminated by the electron beam, to the present work of Poppa^{8,9} in good vacuum ($\sim 10^{-7}$ torr), with defined evaporation rate and no beam contamination. Nevertheless, we have to discuss first the influence of the experimental conditions on the results of in-situ investigations before we can draw any general conclusions on the growth process of thin films in general.

IV. THE INFLUENCE OF THE EXPERIMENTAL CONDITIONS ON THE FILM GROWTH

The main difficulties for a generalization of the results of in-situ investigations are: the influence of (1) the electron beam, (2) the residual gas, and (3) the surface condition and the limited number of film and substrate materials used.

The electron beam can influence the film growth in many ways: by hydrocarbon contamination of the substrate surface or the growing film; by heating; by dissociation of the substrate and/or film material and the residual gas; and by desorption of adsorbed gases. Hydrocarbon contamination can be nearly eliminated by proper heating of the specimen and/or cooling its environment. Specimen heating can be minimized by proper illumination, but nevertheless can be considerable if proper care is not taken. Specimen heating may have been responsible for the reduced condensation of Ge on NaCl,²³ in the electron bombarded area in conventional vacuum and for a similar phenomenon in the condensation of Au on NaCl in ultrahigh vacuum.²⁴ The somewhat slower film growth of Ag on MoS₂ in the electron bombarded area noted by Bassett¹⁵ and Pashley et al.²¹ may also have been due to specimen heating. However rapid dissociation of the substrate surface by the high intensity beam can have the same effect. Dissociation which is limited to compound substrates and films may not only reduce

or increase the rate of film formation but may also influence the orientation of the film crystallites. A reduction of the rate of film formation is observed when the removal of material due to dissociation is comparable with or larger than the deposition rate. This can happen at low condensation rates and high continuous beam intensities. The rate of film formation increases if a compound substrate is irradiated with a high intensity beam only for a small fraction of the condensation time²⁴ or if the electron beam is of low intensity.²⁵ This has been observed, e.g. for Au on NaCl in UHV²⁴ and for Ag on NaCl, mica and MoS₂ in conventional vacuum. The influence of a low intensity electron beam depends considerably upon the residual gas and will be discussed below. On monoatomic substrates no dissociation can occur and the beam influence can be best explained by desorption of adsorbed gases. Such observations have been made for Ag and Sb on carbon.^{8,9} Whatever the details of the influence of the electron beam may be, the liquid like behavior is not caused by it, because coalescence takes place also in films grown without the influence of the electron beam.

There are many indications that residual gases have considerable influence on the growth process, depending upon the nature and pressure of the gas and upon the substrate temperature. This is illustrated by the following example: A discontinuous Pt film deposited in UHV onto mica has a much more uniform and about an order of magnitude larger grain size than a film obtained in a conventional vacuum system. This has been attributed to a lower nucleation rate and higher mobility of the Pt on mica in UHV.²⁷ Continuous Sn and In films deposited at room temperature in UHV or in N₂, H₂, A, CH₄, and CO have a much larger grain size than the same films deposited in a O₂ residual gas atmosphere. The films grown in N₂, H₂, A, CH₄, and CO develop a strong preferred orientation ([100] and [010] fiber texture for Sn and In respectively), while the films grown in O₂

are randomly oriented. In discontinuous films the tendency to coagulate is much larger in UHV than in O_2 , although the films in both cases become electrically continuous at about the same thickness. These observations indicate that O_2 reduces the mobility of the deposited material and inhibits the coalescence of the individual grains.²⁸ NaCl grows on NaCl in He, H_2 , N_2 , O_2 at $180^\circ C$ up to the highest deposition rates ($1000 \text{ \AA}/\text{sec}$) only in parallel orientation; while in the presence of water vapor, CO, CO_2 or C_2H_2 nuclei with $\{110\}$ orientation are formed, and in the presence of C_4H_{10} nuclei in twin orientation are formed. If NaCl is deposited both in the presence of C_4H_{10} and a low intensity electron beam, $\{110\}$ oriented crystals are formed instead of twins.²⁶ These examples indicate that residual gases, with complications due to the electron beam, can strongly influence both nucleation and agglomeration by changing the size, shape and orientation of the crystals both in the discontinuous and in the continuous film. That such effects certainly exist in the in-situ investigations discussed above is indicated by Pashley's et al. observation²¹ that Au grows much more sideways on MoS_2 if deposited in UHV.

Frequently, it is difficult to separate the influence of the residual gas from that of the substrate surface condition: At high residual gas pressure, a surface cleaned, e.g. by heating, ion or electron bombardment is very soon again covered with an adsorbed layer; in UHV the surfaces have frequently lost their adsorbed layer due to the bake-out used to remove adsorbed layers from the walls of the vacuum system. Nevertheless, there are clear indications that at a given residual gas pressure and composition differences in the substrate surface condition can strongly influence film growth. A trivial example is the decoration of water marks in the early states of film growth at low supersaturation. A more sophisticated example is the influence of the surface layer

on alkali halide crystals cleaved in air on the orientation of films deposited onto them which was already noticed by Shirai.²⁹ He found that Fe, Cr, Mo, and Ag films deposited onto NaCl cleavage planes which had been annealed at elevated temperatures (321 - 638°C) before deposition had in general more orientations and a different "epitaxial temperature" than films deposited onto as-cleaved surfaces under otherwise identical conditions. Recently, the influence of the surface state has been demonstrated especially strikingly by the experiments of Ino et al.³⁰ They showed that the "epitaxial temperature" of Ag deposited onto vacuum cleaved NaCl had an "epitaxial temperature" 150°C below that of a film deposited on an air-cleaved surface. We will discuss their results together with that of later related work below. There is little doubt that the surface condition can also have considerable influence on the in-situ results, e.g. due to a reduction of the film-substrate interaction by adsorbed layers.³¹ Poppa²⁰ has given an example for the influence of the surface condition in in-situ experiments, using ion bombardment cleaning.

In all in-situ experiments described above metals were used as film material. Metals are plastic, their surface energy is only weakly anisotropic and many of them have high heats of adsorption for residual gases. To what extent can we expect the results obtained with metals to be valid for ionic crystals which are brittle, which have surface energies varying strongly with direction and which have low heats of adsorption? Early qualitative studies^{7,33} of the growth mechanism of thin films of ionic crystals did not indicate any striking coalescence processes during the merging of crystals as observed with metals. This is shown in Fig. 8 which compares a LiF film on NaCl with a Au film on NaCl in a similar growth stage. This apparent lack of coalescence in fact stimulated the rigid model. More recently however Campbell et al.³⁴ have made some

observations in LiF films on carbon which seem to rule out the applicability of the rigid model not because of coalescence of merging particles, but because of break-up. Figure 9 shows some of their results. The number N' of separated particles first decreases as it should after the maximum of N' --the initial increase of N' has not been observed because of the high deposition rate--but then N' increases again with a simultaneous decrease in the average particle area \bar{f} . This observation clearly indicates that we have to be very careful in the generalization of the results obtained with metals to ionic crystals.

Also generalizations to other substrates than those used in the in-situ experiments have to be done with care. The single crystal substrates used are all strongly anisotropic, have layer structure and cleavage planes with hexagonal or pseudohexagonal symmetry and induce in the film an epitaxial $\{111\}$ orientation (except graphite). The $\{111\}$ orientation is not only favored by the symmetry of the substrate but also by the anisotropy of the crystal itself. The $\{111\}$ surface has the lowest free surface energy of all planes in the f.c.c. lattice and the $\{111\}$ interface between crystal and substrate has the lowest interfacial energy compared to all other planes, assuming the same average mismatch (see below). Therefore the $\{111\}$ orientation provides the minimum energy configuration for a plane parallel slab. If the epitaxial orientation is now a $\{100\}$ orientation--as for most f.c.c. metals on alkali halides--then we have to expect a tendency to formation of a $\{111\}$ orientation. How strong this tendency is depends mainly upon the anisotropy of the surface energy of the crystal and the interfacial energy. As both parameters depend on the residual gas and the substrate surface condition, we will examine now the epitaxy of f.c.c. metals on alkali halides from this point of view.

V. THE EPITAXY OF f.c.c. METALS ON ALKALI HALIDE CLEAVAGE PLANES

Instead of tracing the historical development we will start with the discussion of some of the results which Kunz²⁴ has recently obtained from in-situ UHV electron diffraction studies and of some ideas of the mechanism of film growth which have been stimulated by these results. Afterwards, we will look at previous results in the light of these ideas. Kunz's experiments were performed in a Vacion-Ti getter pumped system with a base pressure of $2 \cdot 10^{-10}$ torr after a 4-hour bakeout at 250°C. Au was evaporated simultaneously at rates between 10 and several 100 Å/min onto air- and UHV-cleaved NaCl heated to 300 - 450°C. The film structure was observed by electron diffraction either continuously, intermittently or after the completion of the evaporation in order to eliminate the influence of the electron beam. Most depositions were made at 360°C because at this temperature the air cleaved surface could be maintained in a condition different from that of the UHV cleaved surface for several hours. At 450°C the air cleaved surface assumed the behavior of the UHV cleaved surface in less than one hour, which was noted previously by Matthews and Grünbaum.³⁵ At 360°C the initial growth of the Au film proceeds on both surfaces in parallel orientation to the substrate (see Fig. 10a). The reflection electron diffraction does not show the slightest indication of a {111} orientation parallel to the substrate. The intensity of the pattern on the UHV cleaved surface is much lower than on the air cleaved surface except if the UHV cleaved surface was bombarded intermittently with electrons. With increasing film thickness well pronounced streaks in the $\langle 111 \rangle$ directions of the reciprocal lattice develop (see Fig. 10b). At a mean thickness of 300 - 400 Å a major change occurs: the spot intensity suddenly decreases while the background becomes much more intense. From this

point on the growth on the UHV cleaved part of the crystal proceeds quite differently from that on the air-cleaved part: on the air cleaved side the film shows a well pronounced epitaxy parallel to the rock salt lattice with a complicated interface structure (Fig. 10c); on the vacuum cleaved side however {111} orientations develop (Fig. 10d). A transmission electron diffraction and microscope examination of the films gives the following additional information: the nucleation probability on the UHV cleaved surface is much smaller than on the air cleaved surface (Fig. 11a, f). With increasing film thickness, crystals in other orientations besides the parallel orientation appear, predominantly randomly and {111} oriented crystals (Fig. 12b, g). Coalescence leads on the UHV cleaved surface, where it is much more pronounced (Fig. 11c, h), to a considerable enhancement of the {111} orientations, mainly at the expense of the parallel orientation (Fig. 12i), while on the air cleaved surface the parallel orientation becomes dominant (Fig. 12c). As a result of these tendencies continuous films on UHV cleaved surfaces consist of large {111} oriented crystals with linear dimensions of the order 1μ (Fig. 11k). Many of them seem to be free of dislocations, producing weak Kikuchi patterns (Fig. 12h), others are full of dislocation tangles. The continuous films on the air cleaved side consist of much smaller crystals in parallel orientation which frequently contain twins (Fig. 11e) or produce clear Kikuchi patterns (Fig. 12h).

These results clearly show that the orientation of the continuous films can be completely different from that of the isolated nuclei and that the crucial stage of the film growth in which the final orientation is determined is the coalescence stage. In the present experiments the only difference in the experimental parameters leading to the two final orientations was in the condition of the substrate surface. As a consequence of this difference, the nucleation

probability was lower and the tendency to coalescence was higher on the vacuum cleaved surface than on the air cleaved surface. The first phenomenon was also noted in conventional vacuum by Sella and Trillat,³⁶ however the second is not observed in conventional vacuum,³⁶ where the coalescence on a vacuum cleaved surface is identical to that on an air cleaved one.³⁷

What distinguishes now the two surface conditions and what is the influence of the residual gas? Bethge et al.^{38,39} and others^{36,40} have studied the structure of air and vacuum cleaved NaCl surfaces and its change under the influence of water vapor using the preferred nucleation at steps ("gold decoration technique")^{36,38-40} and surface conductivity measurement. Although steps do not influence the orientation of Au nuclei, not even in UHV,⁴¹ their configuration can give information on the condition of the surface. From these experiments it has been concluded that an air cleaved NaCl surface interacts with the atmospheric water vapor and recrystallizes into a hydrate like surface structure.³⁹ The rate of formation of this surface structure depends upon water vapor partial pressure. This is used to explain that Au films deposited on UHV cleaved surfaces which had been exposed to water vapor at 10 torr for one hour had the same structure as films grown on clean surfaces, while an exposure to 75 torr (or more) of air for one hour produced films with the same structure as that obtained on an air cleaved surface.³⁵ On the other hand, Harsdorff and Raether⁴² found that the optimum orientation in Ag film evaporated onto NaCl at 60°C is already obtained 8 sec after cleavage in a residual gas pressure of 10^{-6} torr. By changing the residual gas they showed that the gas component most effective in improving the film orientation was water vapor, in agreement with earlier work on the degree of orientation in Cu films on NaCl.⁴³ In this work Harsdorff had found that the degree of orientation of continuous films of Au, Ag, and Cu

on NaCl, KCl, KI had maximum and minima as function of substrate temperature. He associated the maxima with the beginning of evaporation of adsorbed layers.

If this interpretation is accepted six adsorbed layers on NaCl are necessary to explain the data for Ag. Recent mass-spectrometric evidence⁴⁴ seems to confirm the existence of several adsorbed H₂O layers. If a NaCl crystal is slowly heated to 500°C several H₂O desorption peaks are observed at reproducible temperatures. One of them is shown in Fig. 13a. However the peak shape is not compatible with the kinetics of a single desorption process. Mass spectrometric studies by Green⁴⁵ who used NaCl exposed to D₂O in order to distinguish between H₂O on the surface and H₂O in the bulk reproduced the D₂O "desorption peaks"--all shifted to somewhat lower temperature--but showed definitely that they cannot be due to a desorption process (Fig. 13b). We associate the peaks tentatively with burst of D₂O bubbles formed by diffusion of D₂O into the bulk. No such bursts are observed at mass 28 if even the crystals were cleaved in CO and CO₂. The reinterpretation of the "desorption" peaks does not mean that adsorbed H₂O layers do not exist, however much higher heating rates would be required in order to observe their desorption. In fact, the existence of an adsorbed layer is indicated in low energy electron diffraction patterns⁴⁶ of NaCl surfaces exposed to H₂O and baked for several hours at 200°C, which differ from those of surfaces heated to 500°C in a considerably increased background, although they have the same periodicity. If the surface is a monolayer or a multilayer and how the H₂O or OH⁻ is distributed normal to the surface cannot be determined at present. We believe therefore that the nature and thickness of the adsorbed layer necessary for the formation of continuous epitaxial films is still an unsolved problem.

Another open question is to what extent the failure to form an epitaxial film in the absence of the adsorbed layer is due to nucleation or due to

coalescence. We have seen earlier that Au nuclei on a UHV cleaved NaCl surface at 360°C are oriented parallel to the substrate, while with increasing film thickness a {111} orientation develops. The parallel orientation is also prominent in very thin films (10 Å thickness) at lower substrate temperatures down to room temperature, although the amount of {111} orientation increases with decreasing temperature.³⁵ This increase in {111} orientation can easily be explained by coalescence because with decreasing substrate temperature the number of nuclei increases rapidly so that coalescence starts at a much earlier stage of film growth. On the other hand, it could be argued that the experiments performed up to now were not done with clean enough surfaces and that on a really clean surface the Au nuclei would not be oriented. Some of the arguments in favor of such an opinion are: (1) a burst of H₂O is observed if NaCl is cleaved in vacuum at room temperature,⁴⁷ at least a fraction of the H₂O can be adsorbed on the surface of the crystal; (2) when a NaCl crystal is heated, many small⁴⁵ and several large H₂O bursts^{44,45} are observed in the temperature range investigated (up to 500°C). If we attribute the bursts to H₂O coming from the interior of the crystal, then a surface cleaved even in the best vacuum has enough chance to be covered with at least a fraction of a monolayer of adsorbed H₂O supplied from the interior of the crystal even after a prolonged bakeout at several hundred °C. If there is a limited supply of adsorbed H₂O, it can be used up in the formation of the interface of the initially formed nuclei which act as scavengers for adsorbed gases. The initially formed nuclei could thus have parallel orientation, while the nuclei formed later would assume the orientation characteristic for the clean surface. An indication that this might be true is the observation that the Au nuclei on UHV cleaved NaCl at 360°C formed at a later stage of the film growth in the space between the coalesced crystals have

nearly exclusively {111} orientation.²⁴ These considerations show the need for more experiments to understand the elementary processes of the growth of thin films even in a system as extensively investigated as Au on NaCl.

DISCUSSION

We will discuss now some of the most outstanding features observed in the formation of continuous films from isolated nuclei from the theoretical point of view. The most striking phenomenon in metal films is the coalescence of particles, which changes particle size, shape and orientation as compared to that expected from the rigid model. The experiments indicate that the tendency to coalescence depends mainly upon the condition of the substrate surface, the residual gas pressure, the surface energy of the film material and the particle size. This is not surprising if we consider that the system tries to minimize its free energy. When some particles coalesce the decrease in Gibbs free energy is given by

$$\Delta G = \sum_{hkl} \Delta F_{hkl} \sigma_{hkl} + \Delta F^i (\sigma_{h'k'l'}^i - \sigma^s) \quad (8)$$

where ΔF_{hkl} and ΔF^i are the changes in surface and interface areas of the particles respectively, the σ_{hkl} are the specific free surface energies of the exposed surfaces {hkl} of the particles, $\sigma_{h'k'l'}^i$ the specific interface energy and σ^s the specific surface energy of the substrate. The surface is proportional to $g^{2/3}$ (g number of atoms in the particle). Therefore, the free energy gain per atom $\Delta G_{at} = \frac{\Delta G}{g}$ is proportional to $g^{-1/3}$ or $\frac{1}{L}$ where L is a linear dimension of the particle, which explains the decrease in coalescence tendency with particle size. If a very large particle absorbs a very small one the linear dimensions of the small one determine the process because the whole energy is dissipated essentially only in the redistribution of the atoms of the small particle.

According to Eq. (8) $\Delta G \sim \sigma_{hkl}$. Adsorbed gases reduce the surface energy according to the Gibbs adsorption equation by

$$\Delta\sigma_{hkl} = -kT \int_0^{p_0} \Gamma_{hkl}(p) \frac{dp}{p} \quad (9)$$

where p_0 is the pressure of the gas with which the adsorption layer is in equilibrium and $\Gamma_{hkl}(p)$ the surface concentration of the gas of pressure p at the $\{hkl\}$ face. Γ_{hkl} increases with gas pressure and heat of adsorption. Consequently σ_{hkl} decreases. At a given gas pressure Γ_{hkl} is different on different crystal planes. For example $\{100\}$ and $\{110\}$ planes of Cu exposed simultaneously with $\{111\}$ planes ($\sigma_{111} < \sigma_{100} < \sigma_{110}$) to a given oxygen dose are covered with half a monolayer of oxygen, while the $\{111\}$ planes have only a small fraction of a monolayer adsorbed.⁴⁶ Therefore adsorbed gases cannot only reduce the magnitude of the surface energy but also its anisotropy, e.g. the difference between the surface energy of $\{100\}$ and $\{111\}$ planes. As a consequence the decrease in the free energy ΔG due to the change in total surface area $\Delta F = \sum_{hkl} \Delta F_{hkl}$ becomes smaller in the presence of adsorbable gases. Also the free energy change due to the replacement of $\{hkl\}$ faces with larger σ_{hkl} such as $\{100\}$ planes by planes with smaller σ_{hkl} such as $\{111\}$ planes decreases upon adsorption. Consequently the tendency to coalescence decreases. It should be noted that the adsorption layer does not necessarily have to come from the residual gas, it can also come from the substrate. Molecules adsorbed on the substrate can diffuse onto the surface of the particles and be adsorbed there. So can reaction products between film and substrate. This seems to be the case in the epitaxy of Au on KCl.²⁴

While a high particle surface energy favors coalescence, a high substrate surface energy opposes coalescence (see Eq. (8)). Adsorption of molecules

either from the surrounding gas phase or from the bulk of the substrate, will reduce the substrate surface energy and consequently encourage coalescence. For the influence of the interfacial energy on coalescence on non-crystalline substrates the same considerations are valid as for the surface energy. On crystalline substrates, however, the situation is more complicated due to the misfit between film and substrate and due to the elastic anisotropy of the film crystals. This can be seen best using the most popular interface model, van der Merwe's dislocation interface.⁴⁸ For a given substrate surface orientation, the energy of such an interface in the limit of large misfits is

$$\sigma_{hkl}^i \approx \frac{G_{hkl}^* b_{hkl}}{4\pi^2}, \quad (10)$$

where b_{hkl} is a measure for the average misfit and G_{hkl}^* is an interface shear modulus which depends upon the shear moduli G_{hkl} and G^S of the film crystals and substrate respectively. Because of the elastic anisotropy of crystals σ_{hkl}^i varies with crystal orientation not only due to a changing misfit, but also due to a change in G_{hkl}^* . This is indicated in Table III which gives the ratio $\frac{2c_{44}}{c_{11} - c_{12}}$ for NaCl and f.c.c. metals as a measure for the elastic anisotropy, and the shear moduli for shearing of the {111} and {100} planes.

TABLE III

	NaCl	Al	Ni	Au	Ag	Cu	Pb
$\frac{2c_{44}}{c_{11} - c_{12}}$	0.7	1.3	2.5	2.9	3.0	3.2	3.9
G_{111}		2.48	6.08	1.88	1.93	3.05	$.49 \cdot 10^{11}$ dyn/cm ²
G_{100}	1.26	2.82	12.47	4.20	4.37	7.54	$1.44 \cdot 10^{11}$ dyn/cm ²

If the average misfit for a {111} plane of a f.c.c. metal on a crystalline substrate is not much larger than for a {100} plane, and if the strain energy in the f.c.c. crystal is a major part of the total interfacial energy, then $\sigma_{111}^i < \sigma_{100}^i$ and a {111} orientation is more stable than a {100} orientation. This may be the case in Au on clean NaCl. However, if the major part of the interfacial energy resides in an adsorption layer with a small shear modulus between substrate and crystal, then the elastic anisotropy of the film crystal will play little role and the minimum σ^i will be mainly determined by misfit and bonding conditions. This is probably the case for Au on NaCl with an adsorption layer. That misfit and elastic anisotropy considerations alone are not sufficient to explain the orientation of f.c.c. metals on alkali halides is indicated by the fact that Al grows in general in {111} orientation although it has the same lattice constant as Ag and Au and a much smaller elastic anisotropy than the other f.c.c. metals (see Table III). However Al is the only f.c.c. metal with heats of formation of halides larger than those of the alkali metals. This indicates the importance of chemical bonding, the possibility of chemical reaction and the formation of transition layers, even in systems which are not known to alloy, mix or react with each other in the bulk. The existence of such interface layers has been demonstrated very clearly in recent years especially by low energy electron diffraction,⁴⁹ even in systems which are known not to alloy in the bulk like Ag on Cu⁴⁶ or are assumed not to react like Au on NaCl or KCl.²⁴

If we accept the idea that $\sigma_{111}^i < \sigma_{100}^i$ for Au on clean NaCl independent of particle size, then we have to assume that the initial nuclei have a {100} orientation due to scavenging of adsorbed molecules which are incorporated into their interface. However--as we have pointed out some time ago¹--the interfacial energy between a small crystalline particle and a crystalline substrate

is a function of particle size and shape, irrespective of what interface model is used, e.g. a dislocation model (for small to moderate misfit) or a vacancy model (for large misfit) or any other physically reasonable model. This could lead to $\sigma_{100}^i < \sigma_{111}^i$ in small particles, which would account for the change in orientation with film thickness without invoking adsorbed gases.

Coalescence and the change in film orientation seem to us the two most important phenomena during the transition from isolated nuclei to the continuous film. However the oscillatory behavior of the degree of orientation of f.c.c. metals on alkali halides as a function of temperature⁴³ may also have to be attributed to this stage of the film growth. Mass spectrometer experiments⁴⁵ suggest, that Harsdorff's original explanation based on a multilayer of adsorbed H₂O is incorrect. Therefore we have to consider some other possible explanations. The most probable one on basis of the experimental evidence available at present is the following: As indicated by the mass spectrometer H₂O evolves especially rapidly from the bulk of the crystal at specific temperatures T_e. It may at least partially be incorporated into the growing interfaces of the crystals before large scale coalescence occurs and allow the crystals to rotate--as observed for Ag on MoS₂¹²--into the minimum energy position. However some other possible explanations cannot be excluded: (1) H₂O may evolve rapidly enough at the temperatures T_e to aid in the formation of a low energy Ag/NaCl interface for the parallel orientation, leading to preferred nucleation in parallel orientation; (2) the interfacial energy is an oscillatory function of interface size.¹ The interface size of a nucleus increases with temperature. Therefore the degree of orientation of the nucleus is an oscillatory function of temperature. This mechanism requires nucleus sizes incompatible with the generally held views of the size of nuclei. Both (1) and (2) require that the nuclei determine the final orientation of the film, i.e. that they do not rotate

during growth. This is not true for the following explanation: (3) crystals with small misorientations relative to each other may not change their orientation when they make contact. The orientation of the continuous film is therefore determined by the orientation of the individual crystals at the time of contact, which in turn depends in an oscillatory manner on the size of the crystal. As the crystal size is a function of temperature, the orientation of the continuous film is an oscillatory function of temperature. This type of speculative interpretation could be continued for many other experimental observations, but it seems futile until more experimental data are available.

In summary, the broad scale introduction into thin film growth research of UHV techniques and of methods to produce clean surfaces have made necessary a considerable revision of previously held views of the growth of thin films. So have also the use of more sophisticated investigation methods such as in-situ electron microscopy, low energy electron diffraction and mass spectrometry. We have learned that the structure of continuous films may be completely different from that expected on the basis of the structure of the initially formed nuclei, not only in particle size and shape--which was known for some time--but also in orientation. The growth phenomena which follow nucleation have been shown to play a major role in the structure of the continuous film. They are influenced--as nucleation is--to a considerable degree by environmental conditions such as residual gas pressure and composition, substrate surface condition and also condition of the bulk of the substrate (e.g. impurity content). The most striking phenomenon is the coalescence of crystals, at least in metal films. Many of the initial orientations in thin films which have previously been attributed to preferred nucleation^{2,3} and most, if not all of the initial growth orientations,³ may be due to coalescence. We suggest, therefore, to call them "coalescence

orientations". They may be identical with the nucleation orientation like in f.c.c. metals on MoS_2 or mica, or they may be different, like in Au on clean NaCl. This has to be considered if films with a given orientation are to be grown epitaxially. Certain manipulations such as proper pretreatment of the substrate or evaporation in residual gases may have to be used in order to suppress the formation of a coalescence orientation different from the nucleation orientation.

Space has not permitted us to discuss here the formation of continuous non-crystalline films or of crystalline films via a liquid or amorphous phase. This is the subject of other papers at the conference. We also have omitted a discussion of the formation of imperfections although a considerable amount of work has been done on this subject and a large fraction of the imperfections found in continuous films are assumed to have been introduced in the coalescence stage. Our goal was only to illustrate with some examples our present understanding of the formation of continuous films from isolated nuclei and of the particle size and orientation in continuous films. Much more experimental work needs to be done, especially on films of ionic and valence crystals, before we can hope to develop a general theory of the subject of this paper, e.g. by generalizing the rigid model.

ACKNOWLEDGMENTS

This work was supported in part under NASA Contract #R-05-030-001. One of the authors (E. Bauer) wishes to thank the organizers of this Conference for enabling him to be present.

REFERENCES

1. E. Bauer, Z. Kristallogr. 110, 372 (1958).
2. E. Bauer, Trans. 9th Nat. Vacuum Symp. AVS 1962, p. 35.
3. E. Bauer, in Single Crystal Films, ed. M. H. Francombe and H. Sato (Pergamon Press 1964), p. 43.
4. E. Bauer, Bull. Am. Phys. Soc. Series II, 4, 362 (1959); unpublished work.
5. M. Avrami, J. Chem. Phys. 7, 1103 (1939); 8, 212 (1940); 9, 177 (1941).
6. H. Walther, Z. Angew. Phys. 10, 272 (1958).
7. E. Bauer, Z. Kristallogr. 110, 395 (1958).
8. H. Poppa, J. Vacuum Sci. Tech. 2, 42 (1965).
9. H. Poppa, in preparation.
10. G. Hass, Kolloid-Z. 100, 230 (1942).
11. T. A. McLauchlan, R. S. Sennett, and G. D. Scott, Can. J. Res. 28A, 530 (1950).
12. G. A. Bassett, Proc. European Conf. Electron Microscopy, Delft 1960, p. 270.
13. D. W. Pashley and M. J. Stowell, Proc. 5th Internat. Conf. Electron Microscopy, Philadelphia 1962, paper GG-1.
14. H. Poppa, in ref. 13, paper GG-14.
15. G. A. Bassett, Proc. Internat. Symp. on Condensation and Evaporation of Solids, Dayton 1962, p. 599.
16. H. Poppa, Trans. 9th Nat. Vacuum Symp. AVS 1962, p. 21.
17. M. J. Stowell, J. Appl. Phys. 34, 2515 (1963).
18. H. Poppa, J. Appl. Phys. 34, 2518 (1963).
19. A. E. Curzon, private communication.
20. H. Poppa, Z. Naturforsch. 19a, 835 (1964).
21. D. W. Pashley, M. J. Stowell, M. H. Jacobs, and T. J. Law, Phil. Mag. 10, 127 (1964).

REFERENCES (CONT'D)

22. A. K. Green, G. Turner, and E. Bauer, Proc. 5th Internat. Conf. Electron Microscopy, Philadelphia 1962, paper GG-6.
23. O. S. Heavens, Proc. Phys. Soc. B65, 825 (1952).
24. K. Kunz and E. Bauer, in preparation.
25. A. K. Green, cited by E. Bauer, J. Appl. Phys. 34, 2516 (1963).
26. A. K. Green and E. Bauer, J. Appl. Phys., to be published.
27. L. Bachmann, W. H. Orr, T. N. Rhodin, and B. M. Siegel, J. Appl. Phys. 31, 1458 (1960).
28. H. L. Caswell, J. Appl. Phys. 32, 105, 2641 (1961).
29. S. Shirai, Proc. Phys. Math. Soc. Japan 20, 855 (1938); 21, 800 (1939); 23, 12, 194 (1941); 25, 633 (1943).
30. S. Ino, D. Watanabe, and S. Ogawa, J. Phys. Soc. Japan 17, 1074 (1962); 19, 881 (1964).
31. G. W. Sears and J. B. Hudson, J. Chem. Phys. 39, 2380 (1963).
32. E. Bauer, cited by W. F. Koehler, Proc. 5th Navy Science Symp. 1961, ONR-9, p. 782.
33. E. Bauer, Thesis, Munich 1955; Z. Kristallogr. 107, 72, 265 (1956).
34. D. S. Campbell, D. J. Stirland, and H. Blackburn, Phil. Mag. 7, 1099 (1962).
35. J. W. Matthews and E. Grünbaum, Phil. Mag. 11, 1233 (1965).
36. C. Sella and J. J. Trillat, in Single Crystal Films, ed. M. H. Francombe and H. Sato (Pergamon Press 1964), p. 201.
37. G. A. Bassett and D. W. Pashley, J. Inst. Metals 87, 449 (1959).
38. H. Bethge, phys. stat. sol. 2, 775 (1962) (with references to earlier work).
39. H. Bethge and M. Krohn, Coll. Internat. CNRS "Adsorption et Croissance Cristalline", Nancy 1965.

REFERENCES (CONT'D)

40. A. Oberlin and M. Hucher, Coll. Internat. CNRS "Adsorption et Croissance Cristalline" Nancy 1965 (with references to earlier work).
41. E. Grünbaum and J. W. Matthews, phys. stat. sol. 9, 731 (1965).
42. M. Harsdorff and H. Raether, Z. Naturforsch. 19a, 1497 (1964).
43. M. Harsdorff, Solid State Comm. 1, 218 (1963); 2, 133 (1964).
44. R. W. Adam and M. Harsdorff, Z. Naturforsch. 20a, 489 (1965).
45. A. K. Green and E. Bauer, unpublished work.
46. E. Bauer, unpublished work.
47. T. A. Vanderslice and N. R. Whetten, J. Chem. Phys. 37, 535 (1962).
48. J. H. van der Merwe, Proc. Phys. Soc. (London) A63, 616 (1950); J. Appl. Phys. 34, 117 (1963); in Single Crystal Films ed. M. H. Francombe and H. Sato (Pergamon Press 1964), p. 136; this conference.
49. See the reviews by J. J. Lander, this conference; J. J. Lander, Surface Science 1, 125 (1964); E. Bauer, Coll. Internat. CNRS "Adsorption et Croissance Cristalline", Nancy 1965.

FIGURE CAPTIONS

- Fig. 1. The three basic film growth mechanisms: (a) Volmer-Weber mechanism, (b) Frank-van der Merwe, (c) Stranski-Krastanov mechanism.¹
- Fig. 2. (a) Theoretical behavior of number of separated particles N' , differential condensation coefficient k and number of condensed atoms according to a strongly simplified rigid model; N_D particle flux, α bulk condensation coefficient.⁴ (b) Condensation of Hg on polished Ni at -85°C .⁶
- Fig. 3. Replica of an epitaxial LiF film on NaCl at 450°C , particle flux $N_D = 1 \cdot 10^{14} \text{ cm}^{-2} \text{ sec}^{-1}$. Original 60 000:1.⁷
- Fig. 4. Initial growth ($N' < N'_{\text{max}}$) of Ag on amorphous carbon at 425°C , particle flux $N_D = 2.5 \cdot 10^{13} \text{ cm}^{-2} \text{ sec}^{-1}$.⁸
- Fig. 5. Growth and coalescence of Ag on mica at 450°C , deposition rate approximately $50 \text{ \AA}/\text{min}$.²⁰
- Fig. 6. Several stages of the coalescence of Ag on MoS_2 .²⁰
- Fig. 7. The influence of the surface condition: Ag simultaneously evaporated onto a boron nitride single crystal flake and amorphous carbon at 400°C .³²
- Fig. 8. The agglomeration stage on ionic films LiF on KBr at 300°C .^{33,7} Original 30 000:1.
- Fig. 9. The growth of LiF on amorphous carbon at room temperature.³⁴ N' number of separated crystals, \bar{f} average crystal cross-section, F fraction of surface covered.

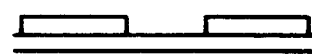
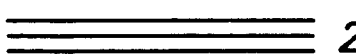
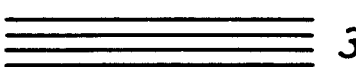
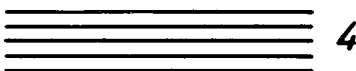
FIGURE CAPTIONS (CONT'D)

Fig. 10. In-situ reflection electron diffraction patterns of Au films grown on NaCl in UHV at 360°C and approximately 50 Å/min. $\langle 110 \rangle$ azimuth of NaCl. Approximate thickness: (a) 10 Å, (b) 100 Å, (c) and (d) thick films (> 500 Å), (c) air cleaved surface, (d) UHV cleaved surface.²⁴

Fig. 11. Electron micrographs of Au films of varying thickness grown on NaCl in UHV at 360°C and approximately 50 Å/min. (a)-(e): air cleaved surface; (f)-(k): UHV cleaved surface. Original 20 000:1.²⁴

Fig. 12. Transmission electron diffraction patterns of Au films of varying thickness grown on NaCl at 360°C and approximately 50 Å/min. (a)-(d): air cleaved surface; (e)-(h): UHV cleaved surface, (f): 10 Å of Au, stabilized with Al on UHV cleaved surface.²⁴

Fig. 13. A typical water peak in the gas evolution during the heating of NaCl crystals. (a) according to,⁴⁴ (b) according to.⁴⁵



a)

b)

c)

Fig. 1

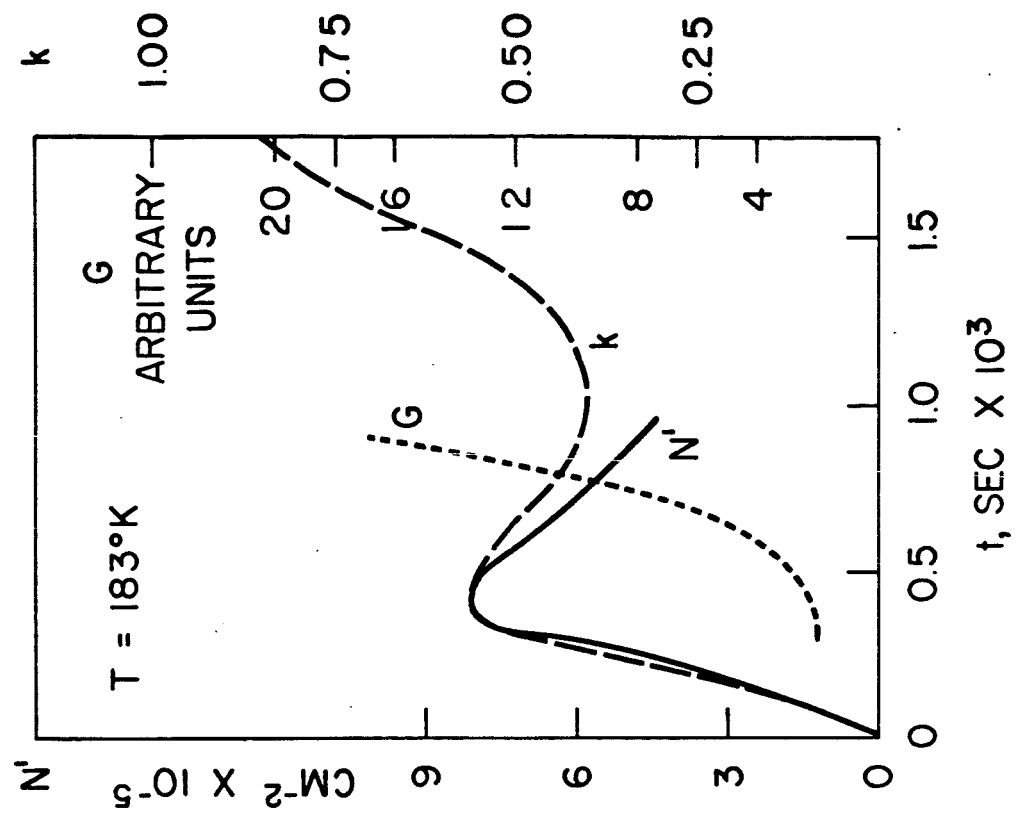
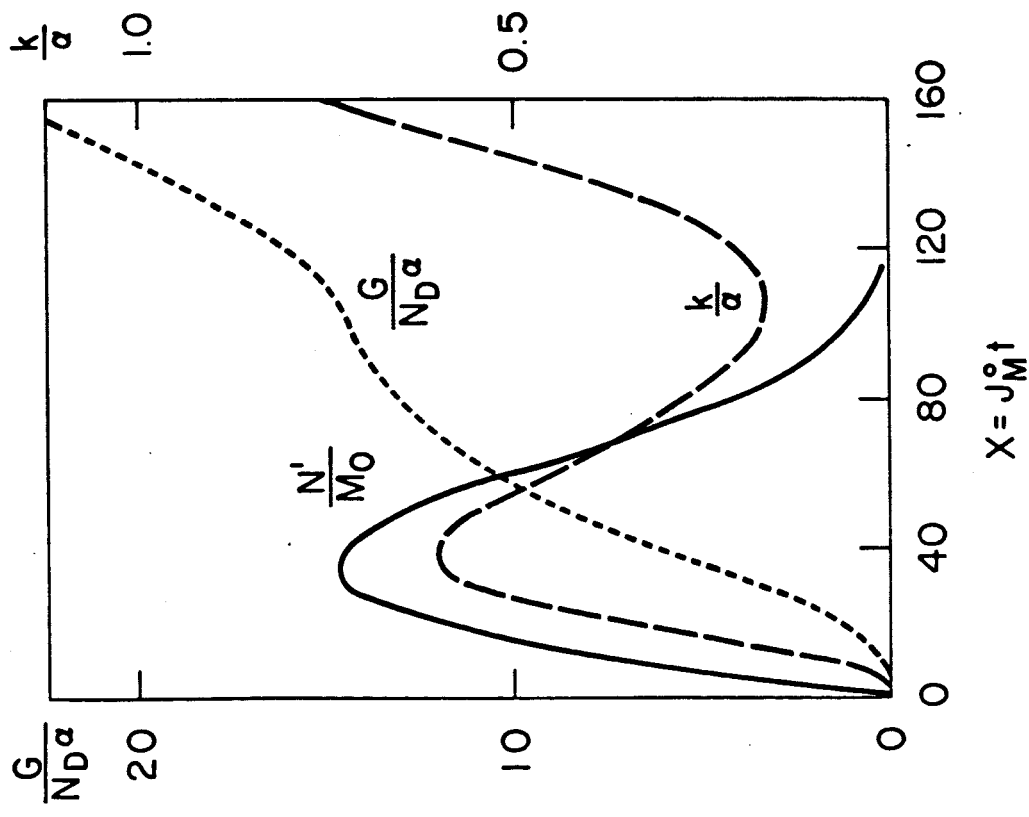


Fig. 2

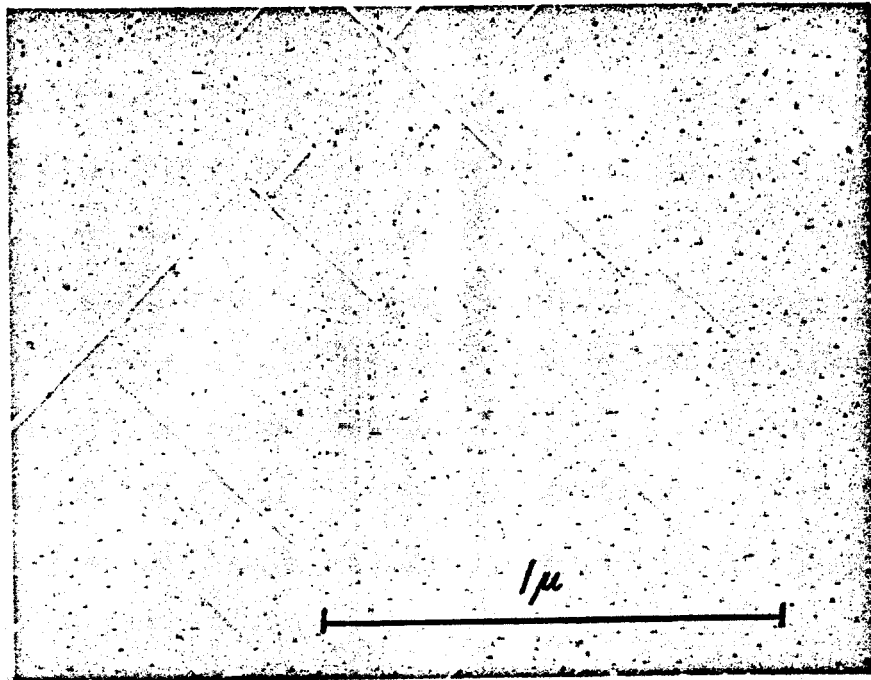


Fig. 3

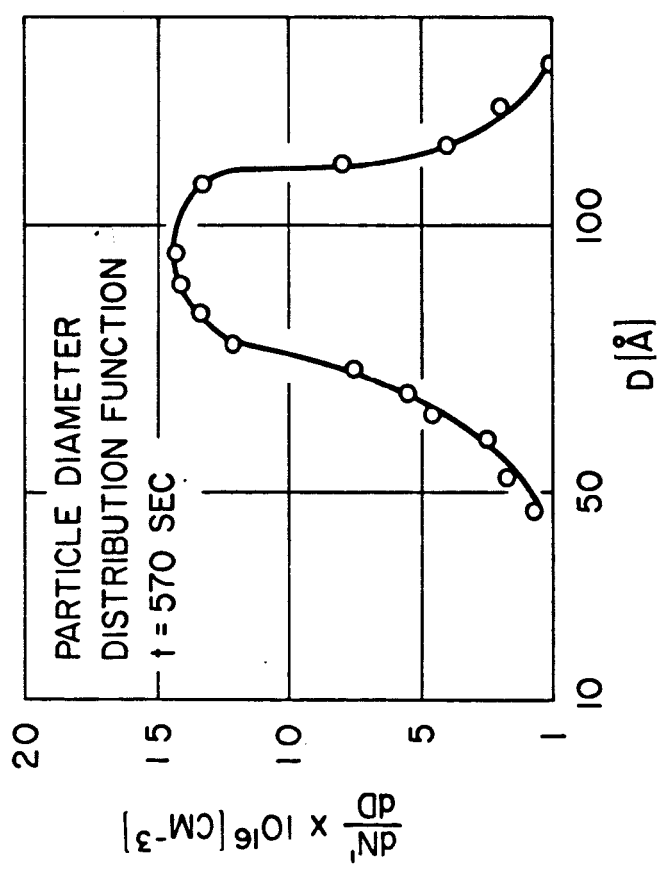
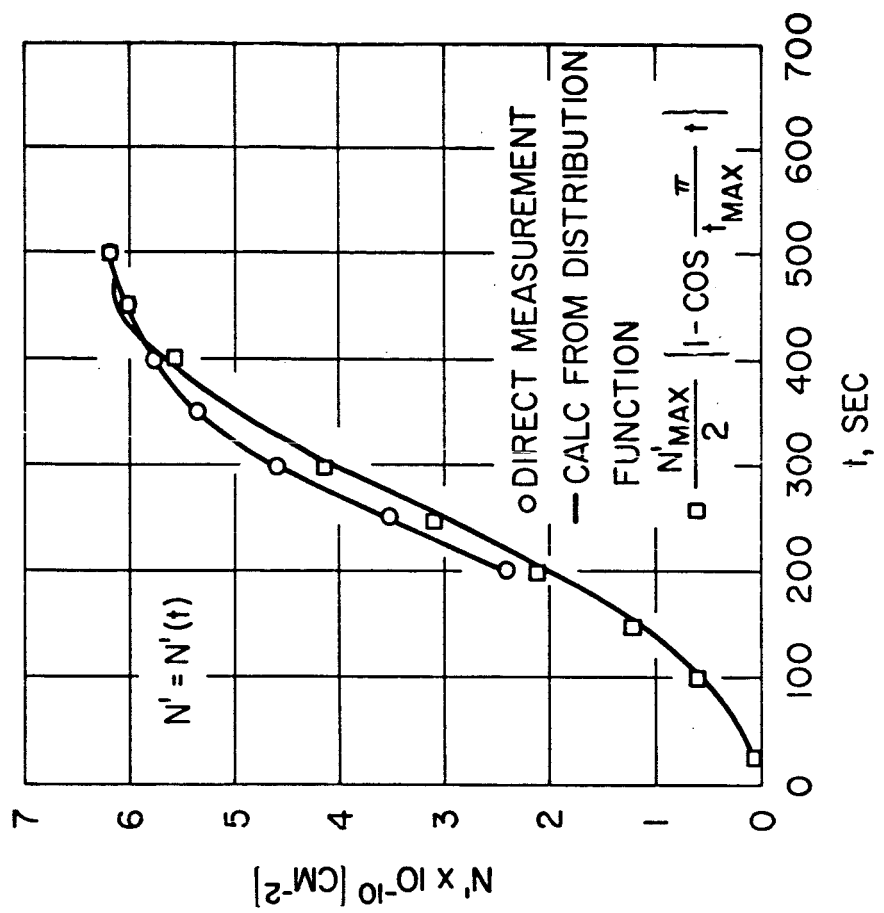


Fig. 4

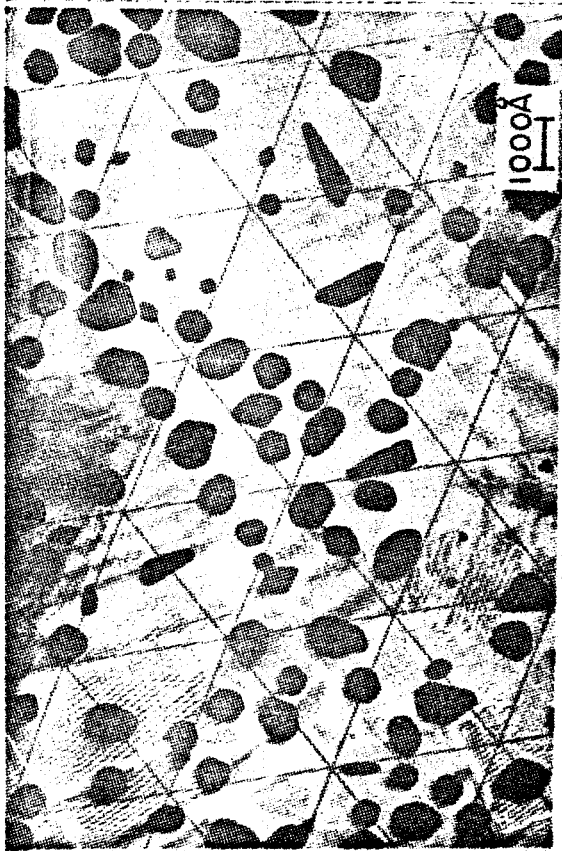
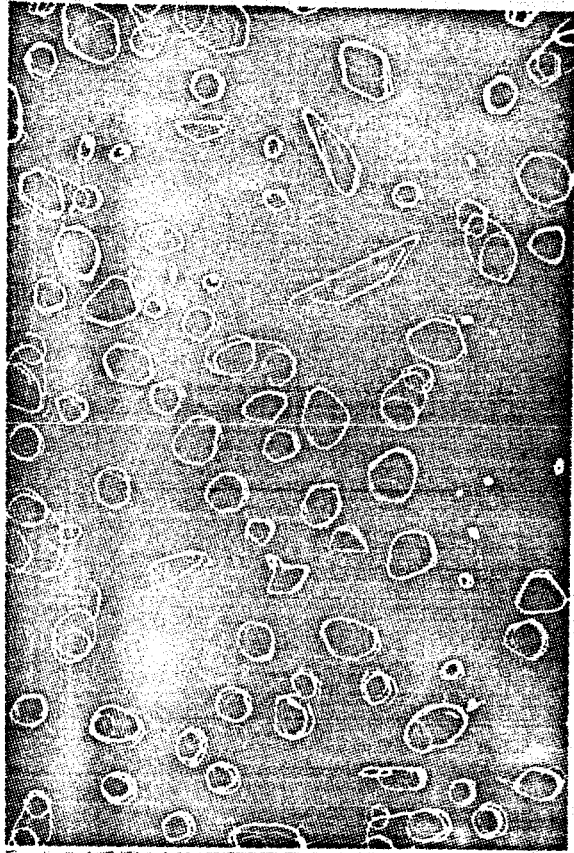
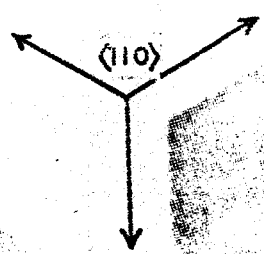


Fig. 5

Fig. 6



100Å



Fig. 7



Fig. 8

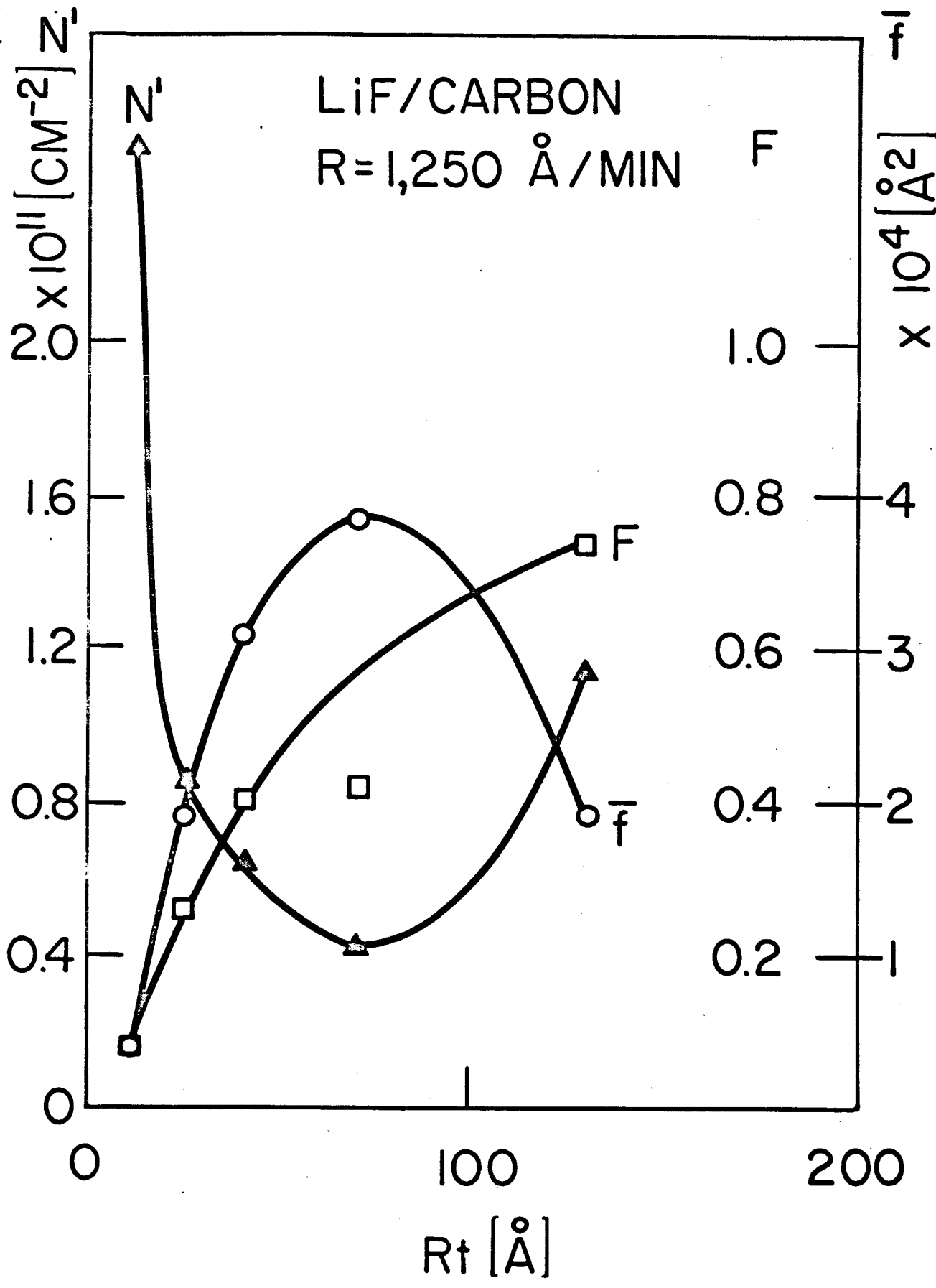
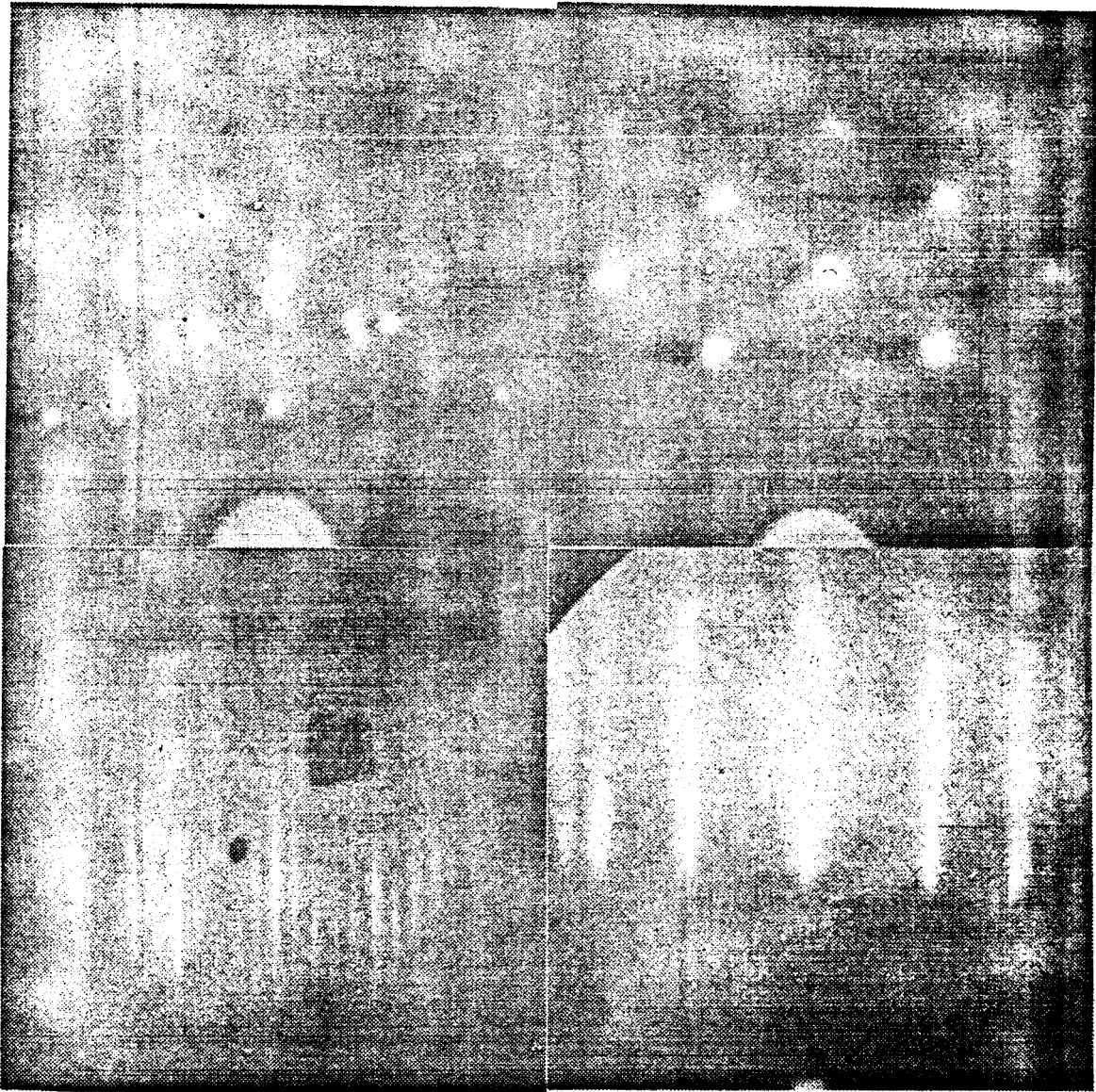


Fig. 9

a

b

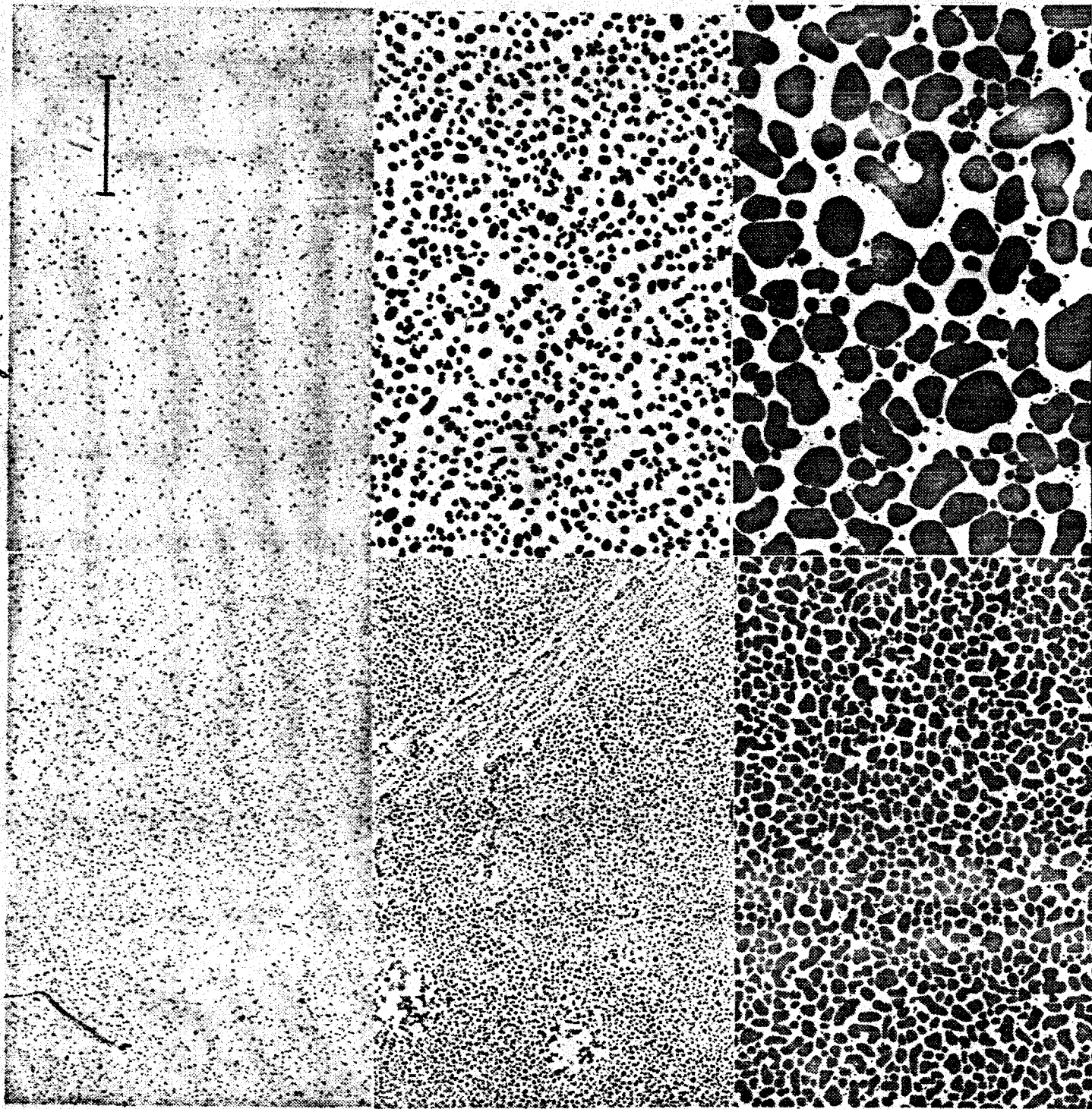


c

d

Fig. 10

Fig. 11





2

R

Fig. 11

P

2

f

R

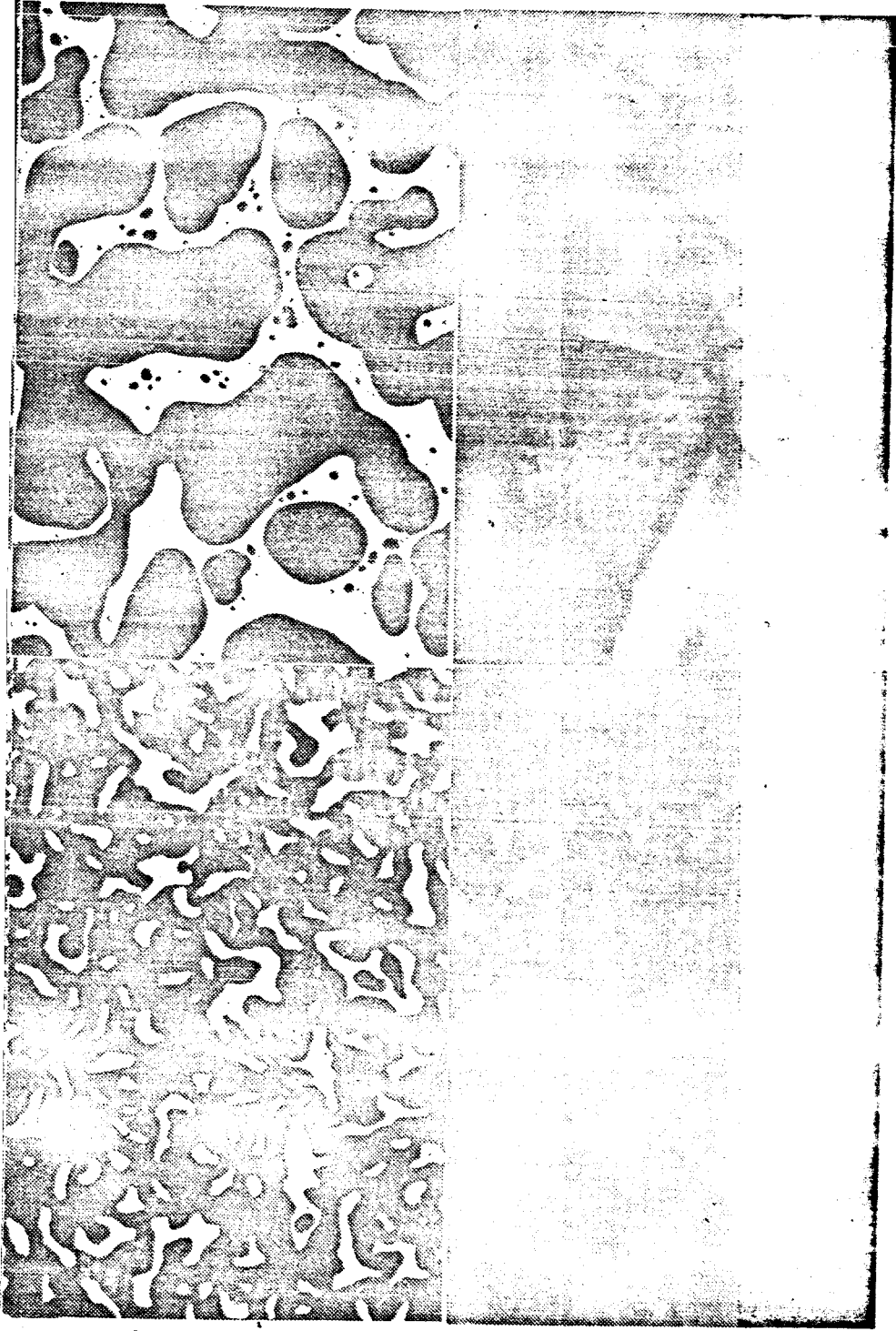


Fig. 11

r

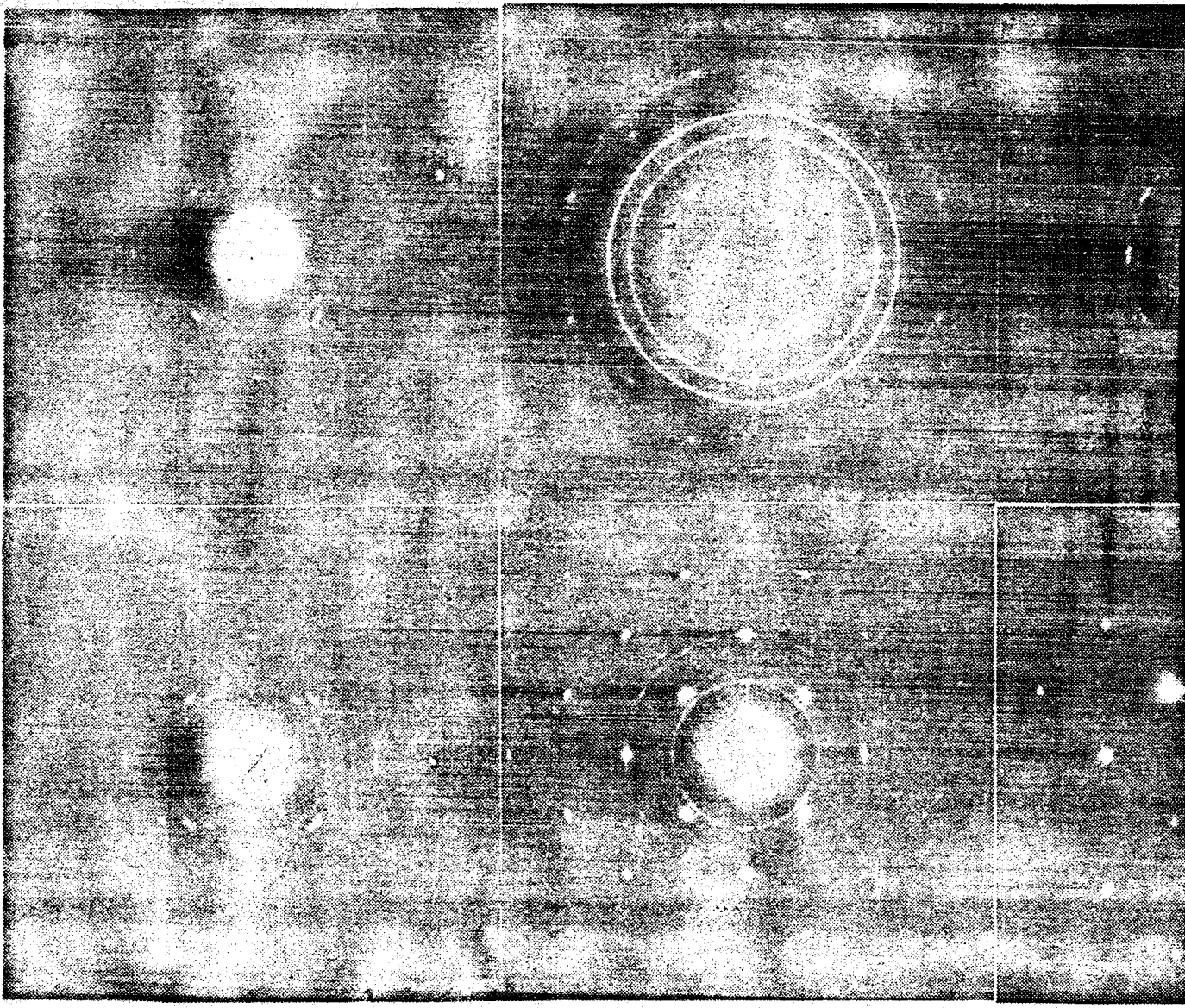
p

1

e

f

Fig. 12



a

b

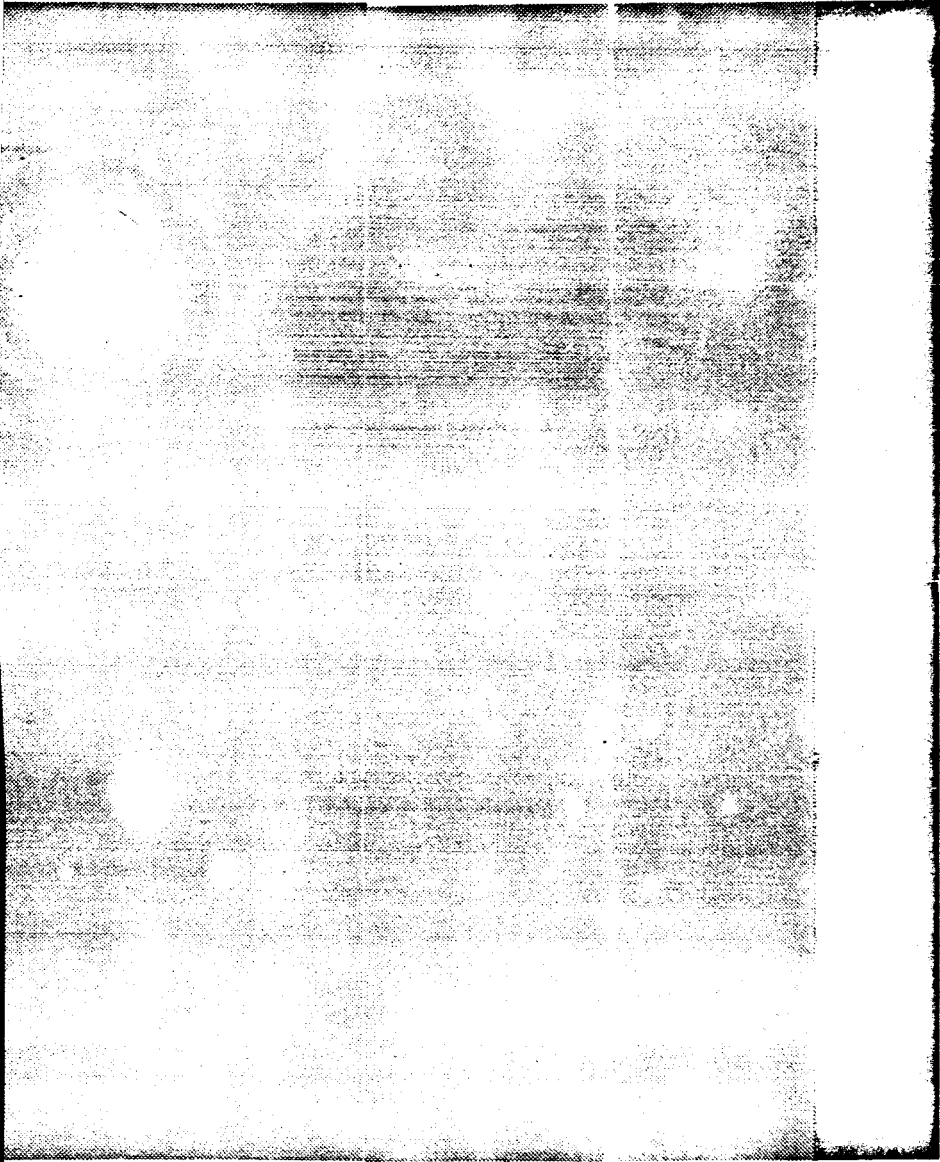


Fig. 12

2

6

4

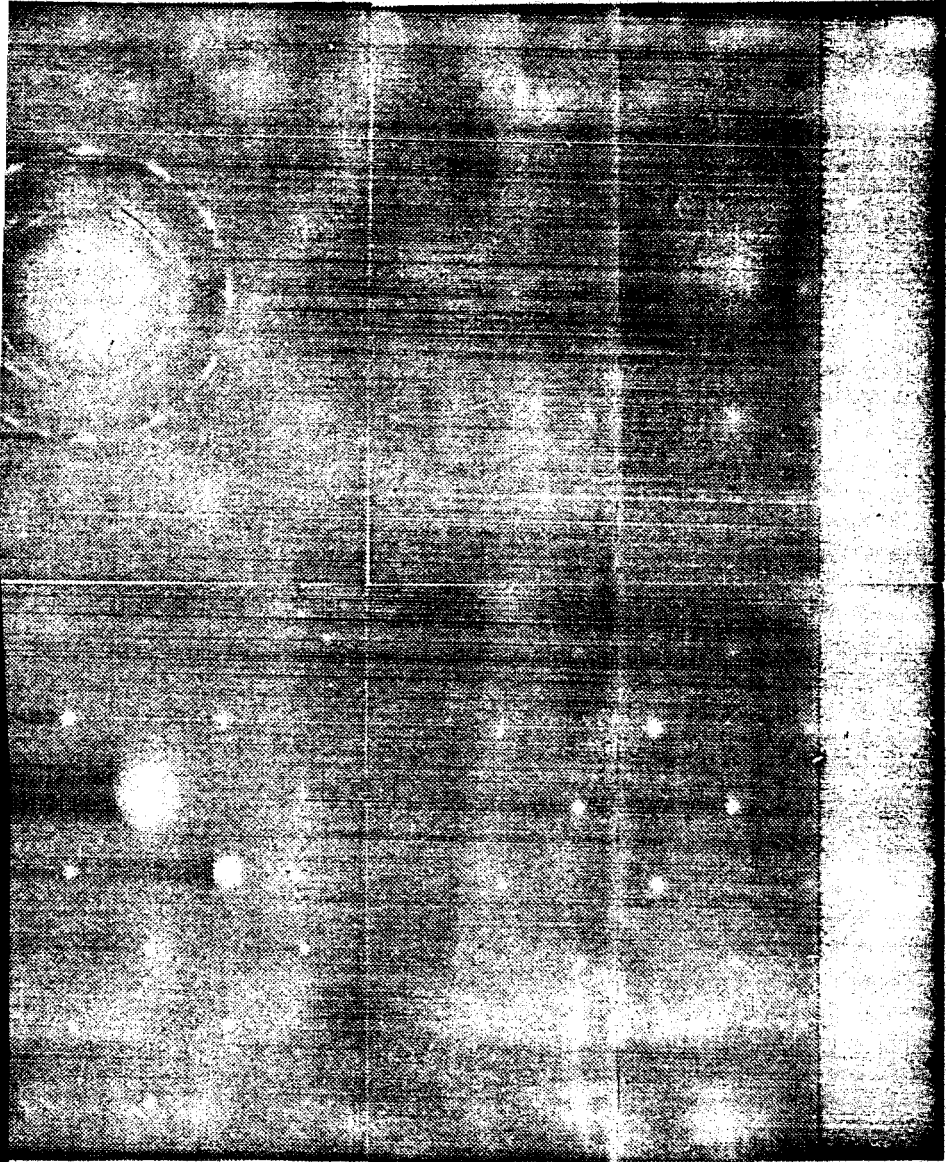
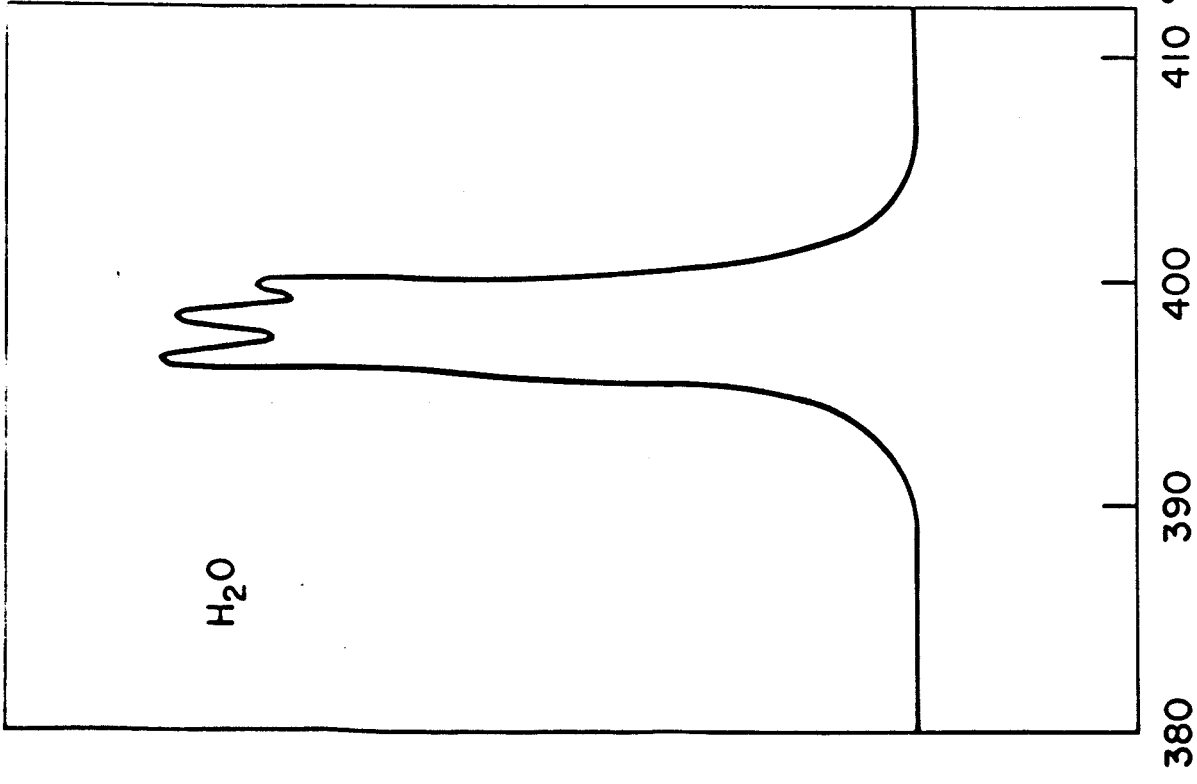


Fig. 12

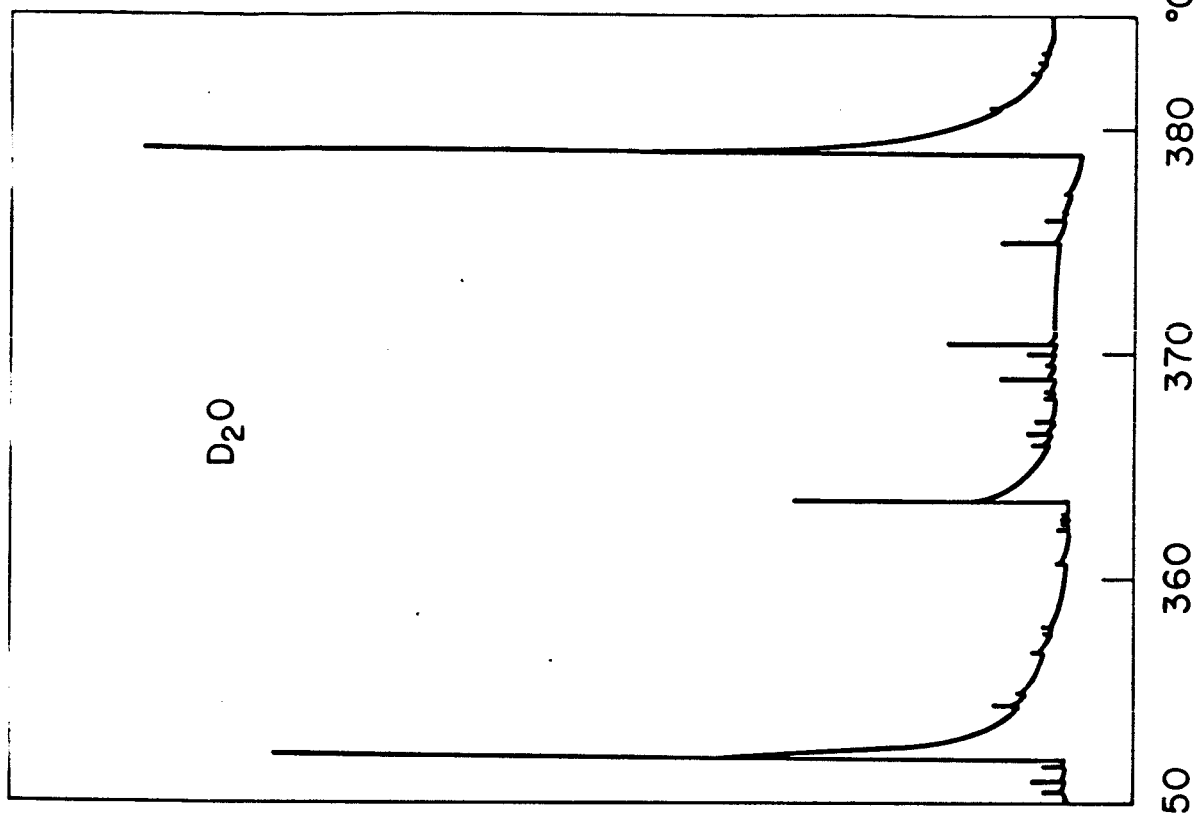
2

2

d



ADAM AND HARS DORFF



GREEN AND BAUER

Fig. 13